IOP FTC
IOP PUBLISHING
JOURNAL OF PHYSICS D: APPLIED PHYSICS
J. Phys. D: Appl. Phys. **43** (2010) 152001 (5pp)
doi:10.1088/0022-3727/43/15/152001

FAST TRACK COMMUNICATION

Graded conductivity electrodes as a means to improve plasma uniformity in dual frequency capacitively coupled plasma sources

Yang Yang[1,3] **and Mark J Kushner**[2,4]

[1] Iowa State University, Department of Electrical and Computer Engineering Ames, IA 50011, USA
[2] University of Michigan, Department of Electrical Engineering and Computer Science 1301 Beal Avenue, Ann Arbor, MI 48109, USA

E-mail: yangying@iastate.edu and mjkush@umich.edu

Received 28 February 2010, in final form 5 March 2010
Published 30 March 2010
Online at stacks.iop.org/JPhysD/43/152001

Abstract
Dual frequency, capacitively coupled plasma (DF-CCP) tools are now being used for etching of 30 cm diameter wafers during microelectronics fabrication. These tools typically use a high frequency (HF, tens to hundreds of megahertz) to sustain the plasma and a low frequency (LF, a few to 10 MHz) for ion acceleration into the wafer. With an increase in both the HF and the wafer size, electromagnetic (EM) wave effects can significantly affect power deposition and the distribution of the plasma due to constructive interference at the centre of the wafer. Here we report on a computational demonstration of using graded conductivity electrodes (GCEs) to improve the plasma uniformity in a DF-CCP reactor. GCEs consist of a metal electrode covered by a dielectric which is in direct contact with the plasma. The conductivity of the dielectric decreases from edge to centre. So as the HF wave propagates inwards from the edge of the electrode, the penetration of the HF field into the dielectric increases. This increasing penetration counteracts the increase in the electric field resulting from the constructive interference of the EM wave at the centre of the reactor, and hence improves the uniformity of the resulting plasma.

Dual frequency capacitively coupled plasma (DF-CCP) reactive ion etching tools are being widely used for plasma etching of dielectrics on large-area substrates [1, 2]. Typically in a DF-CCP reactor, power is applied at a lower radio frequency (rf) to the bottom electrode (a few megahertz to 10 MHz) holding the wafer; and higher frequency power is applied to the top electrode (tens of megahertz to hundreds of megahertz) [3]. Power at the low frequency (LF) is intended to control the shape of the ion energy distributions (IEDs) to the wafer. Power at the high frequency (HF) is intended to control the production of ions and radicals, and hence the magnitude of their fluxes to the substrate. (In some variants, both frequencies are applied to the lower electrode [4]). In order to obtain separate control of IEDs and magnitude of fluxes, a large separation between the LF and the HF is usually required to prevent nonlinear interactions between the two rf sources [5].

As the effective plasma shortened wavelength of the applied HF decreases with increasing frequency and

[3] Present address: Applied Materials Inc., 974 E. Arques Avenue, Sunnyvale, CA 94085, USA.
[4] Author to whom any correspondence should be addressed.

 © 2010 IOP Publishing Ltd Printed in the UK & the USA

approaches the size of the wafer, finite wavelength effects become increasingly important in determining the uniformity of the plasma [5–8]. These effects include constructive and destructive interference and skin effects. For example, the applied electric potential from the cable feed at the rear of the electrode must propagate around the edges of the electrode to enter the plasma, after which the resulting electric field is wave-guided in the sheath at the surface of the electrode. Constructive interference of counter-propagating waves from opposite sides of the electrode increases the amplitude of the electric field in the sheath at the centre of the electrode. This results in a centre-high plasma density.

Methods to suppress these wave effects and improve the plasma uniformity have been proposed. For example, Schmidt *et al* fabricated a Gaussian-shaped surface profile on the powered electrode covered with a thin dielectric plate to confine the plasma in a constant inter-electrode gap [9]. A portion of the larger amplitude of the applied wave at the centre of the electrode was contained within the cavity, leaving a smaller amplitude of the electric field in the sheath, thereby reducing the centre-high plasma density. Separately powered, segmented electrodes have also been proposed to achieve uniform excitation and are used in large area plasma processing for liquid crystal display panels and solar cells [10].

Here, we computationally demonstrate a method to suppress finite wavelength effects and hence improve plasma uniformity in DF-CCP reactors by grading the conductivity of the surface of the electrode in contact with the plasma. The HF metal electrode is shielded from the plasma with a layer of lossy dielectric, the conductivity of which decreases from the edge to the centre of the electrode. So as the HF electromagnetic (EM) wave propagates around the electrode and travels inwards along the surface of the dielectric, the penetration of the HF field into the dielectric increases due to the decreasing conductivity. This leaves a smaller fraction of the potential to be dropped across the sheath. This counteracts the constructive interference of the HF electric field at the centre of the reactor, thereby increasing the uniformity of the HF field. We call this arrangement a graded conductivity electrode (GCE). The system we used to demonstrate the impact of GCE on uniformity is an argon plasma sustained in a DF-CCP with a HF of 150 MHz and LF of 10 MHz. Being aware of the extreme sensitivity of wave propagation to the details of reactor design, such as properties of the materials and process variables such as gas composition and power, we acknowledge that the designs presented here are conceptual. They would likely need further tuning for applications under industrial operating conditions [8].

The model used in this investigation is the two-dimensional (2D) Hybrid Plasma Equipment Model (HPEM). A full-wave solution of Maxwell's equations is integrated into our model to enable simulation of the inductive and finite wavelength effects that result from wave penetration at HF into plasmas, in addition to the electrostatic (ES) effects generally accounted for when solving Poisson's equation. To capture the HF heating, excitation rates are provided by spatially dependent electron energy distributions generated by an electron Monte Carlo simulation (EMCS). The model is described in detail in [11].

In our full-wave Maxwell solution, we separately solve for the EM and ES fields and sum the fields for plasma transport. In 2D cylindrical coordinates, for TM mode propagation, Faraday's law and Ampere's law can be written as

$$\frac{\partial E_r}{\partial z} - \frac{\partial E_z}{\partial r} = -\frac{\partial B_\theta}{\partial t}, \tag{1}$$

$$-\frac{\partial B_\theta}{\partial z} = \mu J_r + \varepsilon\mu\frac{\partial E_r}{\partial t}, \tag{2}$$

$$\frac{1}{r}\frac{\partial (rB_\theta)}{\partial r} = \mu J_z + \varepsilon\mu\frac{\partial E_z}{\partial t}, \tag{3}$$

where J_r and J_z are the radial and axial components of the conduction current, μ is the permeability and ε is the permittivity. The solutions of equations (1)–(3) resolve the EM fields from rf sources. Equations (1)–(3) are discretized on a staggered mesh using the unconditionally stable Crank–Nicholson scheme and solved using finite difference time domain (FDTD) techniques [12]. The current terms in equations (2) and (3) contain contributions from the fluxes of electrons and of ions. The electron flux is computed using a drift–diffusion approximation which contains the term $\sigma\vec{E}$, where σ is the electron conductivity. Implicitness is therefore achieved by the dependence of the electron flux on the electric field through this term. Ion fluxes are given by the solution of their respective ion momentum equations from the previous time step and are held constant during the solution of equations (1)–(3). Poisson's equation for the ES potential is separately solved using the semi-implicit technique described in [11].

Similar to the radiation source from antennas, we define boundary conditions for electric fields for equations (1)–(3) at the locations where the power cables are connected to the reactor. The source electric field is then given by $E(t) = V(t)/d$, where $V(t)$ is the time dependent voltage drop between the centre conductor and the ground shield of the cable connected to the reactor and d is the spacing between them. The boundary conditions for potential on the powered electrodes for the ES solution are either the self-developed dc bias or any applied dc voltages. The amplitudes of applied rf voltages are adjusted to deliver a specified power.

The model reactor used is schematically shown in figure 1(*a*). The base case uses a metal substrate powered at the LF (10 MHz) through a blocking capacitor. A conductive Si wafer ($\sigma = 0.01\,\Omega^{-1}\,\mathrm{cm}^{-1}$), 30 cm in diameter, sits in electrical contact with the substrate which is surrounded by a Si ring (focus ring 1, a dielectric constant $\varepsilon_r = 12.5$, $\sigma = 10^{-6}\,\Omega^{-1}\,\mathrm{cm}^{-1}$), a dielectric focus ring (focus ring 2, $\varepsilon/\varepsilon_0 = 8.5$, $\sigma = 10^{-8}\,\Omega^{-1}\,\mathrm{cm}^{-1}$). The HF electrode consists of a metal plate covered by a dielectric plate having three segments (either made of dielectrics or metal) which are 0.5 cm in thickness. For the purposes of this simulation, these surfaces also serve as the showerhead. The HF electrode is 34 cm in diameter and powered at 150 MHz. A dielectric having $\varepsilon/\varepsilon_0 = 1.0$ surrounds the HF electrode to simulate room air. All other surfaces in the reactor are grounded metal including the annular pump port. The operating conditions are 50 mTorr

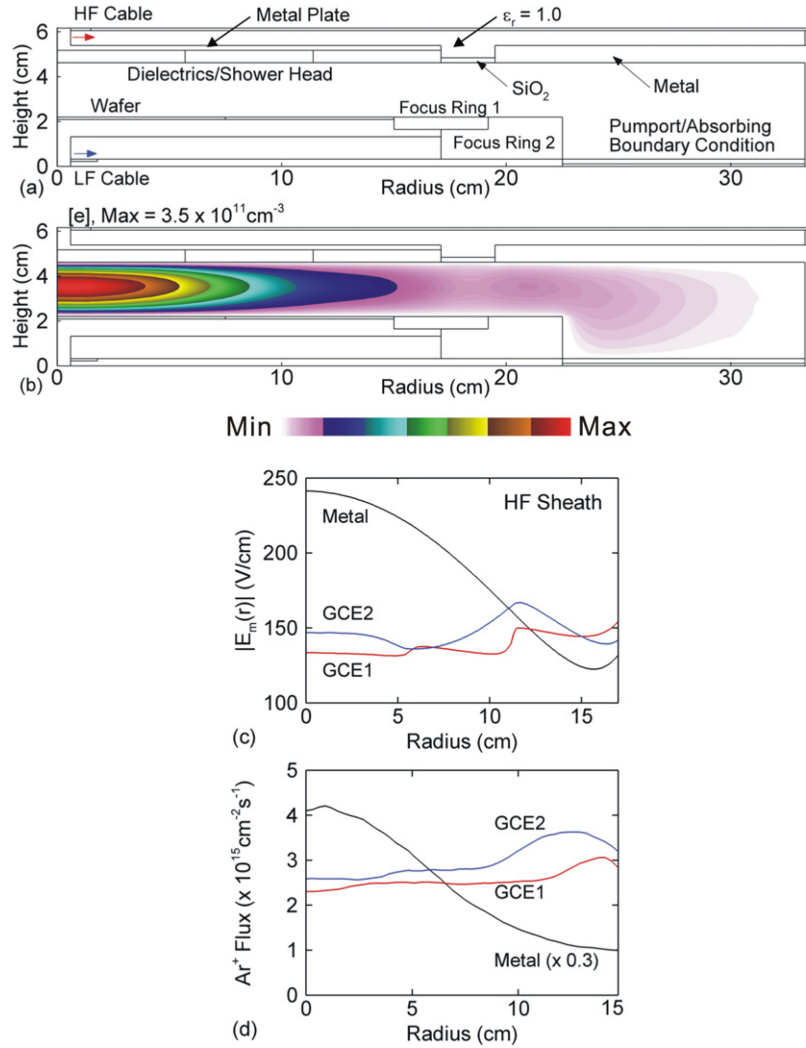

Figure 1. Geometry and plasma properties for Ar, 50 mTorr, $P_{\text{HF}} = P_{\text{LF}} = 300$ W, HF = 150 MHz, LF = 10 MHz. (*a*) Geometry. (*b*) LF rf cycle averaged electron density with a metal electrode. The maximum value of the contour plot is noted. (*c*) Magnitude of the HF electric field along the top sheath for the metal electrode, GCE1 and GCE2. (*d*) Ar^+ flux incident onto the wafer for the metal electrode, GCE1 and GEC2.

of Ar with a flow rate of 400 sccm. The LF power (P_{LF}) and HF power (P_{HF}) are held constant at 300 W, respectively, by adjusting source voltages. The reaction mechanism for Ar is discussed in [13].

With a conventional metal electrode and a HF of 150 MHz, the electron density usually peaks at the centre of the reactor due to the shortening of the plasma wavelength [7, 8]. For example, the LF rf cycle averaged electron density ([e]) is shown in figure 1(*b*) for a metal electrode. The magnitude of the HF field in the HF sheath (relative to the centre of the wafer) is plotted as a function of radius in figure 1(*c*). Note that our model computes the EM field in the time domain, after which a Fourier transform is performed at the HF to obtain the phase change and magnitude of the first harmonic. At 150 MHz, the plasma shortened effective quarter-wavelength is commensurate with the electrode radius, and the HF field is centre peaked from the constructive interference of counter-propagating waves at the centre of the reactor [6]. Since at 150 MHz, electron heating is dominated by stochastic sheath acceleration, the [e] peaks at the centre of the reactor where the sheath electric field is the largest, producing a centre peaked ion flux to the wafer, as shown in figure 1(*d*).

An example of a GCE electrode (GCE1) is shown in figure 2(*a*), where the three segments are made of p-Si ($\varepsilon/\varepsilon_0 = 12.5$). The conductivities of the outermost, middle and central segments are 0.05 Ω^{-1} cm^{-1}, 0.0015 Ω^{-1} cm^{-1} and 0.001 Ω^{-1} cm^{-1}, respectively, thereby presenting a gradient in conductivity in the radial direction. The HF field constructively interferences at the centre of the reactor to produce a maximum in the electric field in the sheath. With the conductivity of the surface layers lowest at the centre of the reactor, the local electric field penetrates deeper into the dielectric at the centre of the electrode, as shown in figure 2(*b*). This consumption of electric potential in the dielectric reduces the voltage that could be expended in the sheath and hence reduces the HF electric field in the sheath at the centre of the reactor. As such, the HF electric field in the sheath is radially more uniform than with a metal electrode, as shown in figures 2(*b*) and 1(*c*).

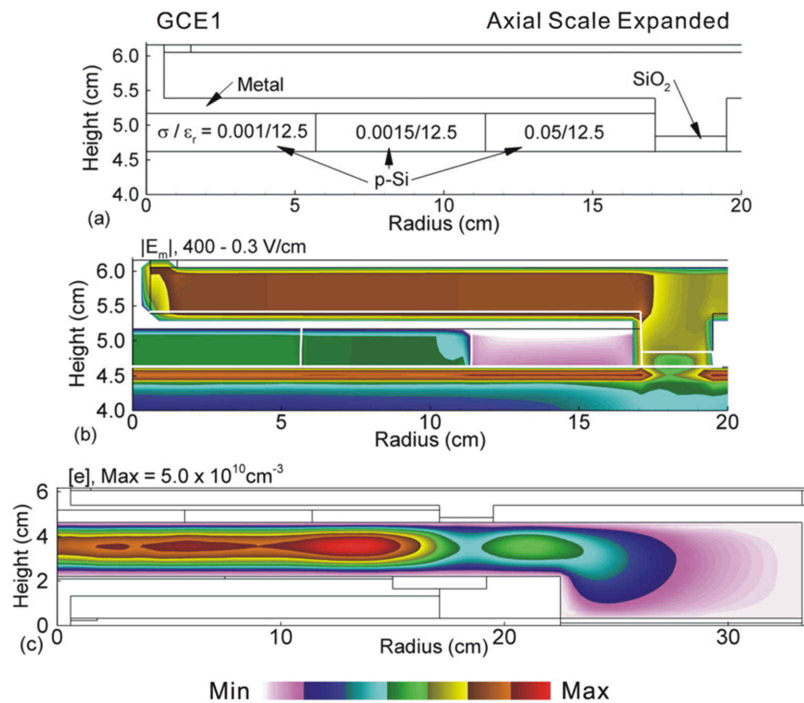

Figure 2. Geometry and plasma properties with the graded conductivity electrode GCE1. (*a*) The HF metal electrode is covered by three p-Si segments with decreasing conductivity from edge to centre of 0.05, 0.0015 and 0.001 Ω^{-1} cm^{-1}. (*b*) Magnitude of the HF field ($|E_m|$) near the top sheath. The $|E_m|$ is plotted on a log scale. (*c*) LF cycle averaged electron density. The maximum value or range of values in each frame of the contour plots are noted.

The centre-to-edge ratio of the HF electric field is less than 1.2, albeit with sharp transitions corresponding to the boundaries between electrode segments. Correspondingly, the [e] and Ar^+ flux onto the wafer (figures 2(*c*) and 1(*d*)) are more uniform compared with the case using the metal electrode. One potential downside of GCEs is heating of the dielectric. For our operating conditions, the central segment of GCE1 dissipates about 57 W, so additional cooling of the electrode may be necessary.

One extension of the design of GCEs is to cover the metal electrode with multiple layers of dielectrics to obtain finer control of the plasma. One such example (GCE2) is shown in figure 3(*a*). A dielectric plate (nominally alumina with $\varepsilon/\varepsilon_0 = 8.0$ and $\sigma = 10^{-8}$ Ω^{-1} cm^{-1}, radius $L = 11$ cm) is sandwiched between the conductive dielectric surface layer and the metal electrode to provide an additional channel for wave propagation. The conductivities of the central and outer segments of the plasma facing layer are 0.005 Ω^{-1} cm^{-1} and 0.05 Ω^{-1} cm^{-1}, respectively. With the conductivity of the surface layer lowest at the centre of the reactor, the HF wave penetrates through the central segment into the dielectric plate and then propagates outwards, being wave-guided by the dielectric plate. As the HF wave cannot penetrate through the outer segment (the most conductive), the wave reflects and diffracts at the periphery of the dielectric plate. Downward propagation then results which enhances the local HF electric field. The HF electric field (figure 1(*b*)) and [e] (figure 3(*c*)) therefore peak near the periphery of the dielectric plate. The ion flux to the wafer is also improved compared with the metal electrode (figure 1(*d*)). Compared with GCE1, the design of GCE2 allows for less lossy dielectrics, which reduces electrode heating. With GCE2, the central segment dissipates about 12 W for these operating conditions.

Designs such as GEC2 allow tailoring the radial position of the maximum in [e] by adjusting the radius of the dielectric plate, L. For example, by decreasing L from 11 to 6 cm, the position of the maximum in [e] moves inwards, as shown in figure 3(*d*). (Note that the intent here is not to optimize uniformity but to demonstrate the ability to manipulate the plasma by using electrode structures.)

Adding additional channels for wave propagation has been previously investigated. Koshiishi *et al* experimentally demonstrated that by making a resonant cavity in the upper electrode (powered at 60 MHz) in a 200 mm DF-CCP reactor, the etching uniformity could be improved [14]. Here, due the higher HF and shorter wavelength, the dielectric plate behaves more like a waveguide, as opposed to a resonant cavity.

In conclusion, we computationally investigated the use of GCEs to improve plasma uniformity in a DF-CCP reactor where constructive interference of the applied electric field produces a centre-high plasma density. By covering the HF metal electrode with a layer of dielectric whose conductivity decreases from edge to centre, the radial uniformity of the HF electric field in the sheath is improved by capturing some of the electric potential of the wave in the dielectric, thereby leaving a smaller potential and electric field in the sheath. Adding an additional layer of dielectric between the metal electrode and the conductive plasma facing dielectric layer provides a channel for wave propagation. Downward propagation of the HF wave at the periphery of the dielectric plate produces a peak

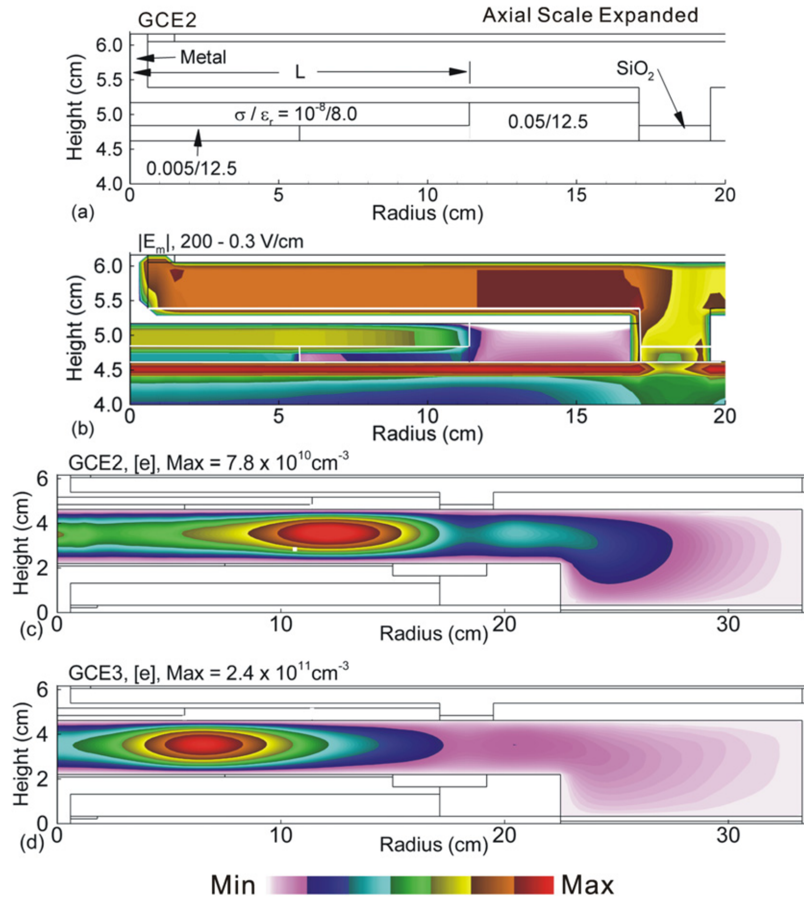

Figure 3. Geometry and plasma properties with GCEs having an intervening dielectric plate. (*a*) Geometry for GCE2 with radius of the dielectric plate $L = 11$ cm. The centre and outer segments of the plasma facing dielectric have $\sigma = 0.005$ and $0.05\ \Omega^{-1}\ \mathrm{cm}^{-1}$. (*b*) Magnitude of the HF field ($|E_m|$) from the cable feed, through the electrode structure and in the sheath for GCE2 having $L = 11$ cm. (*c*) LF rf cycle averaged electron density for GCE2. (*d*) Electron density for GCE3 having $L = 6$ cm. The maximum value or range of values in each frame of the contour plots is noted.

in [e]. Therefore the position of the peak [e] can be tailored by adjusting the radius of the dielectric plate.

Acknowledgments

This work was supported by the US Department of Energy Office of Fusion Energy Science Contract DE-SC0001939, Semiconductor Research Corp., Applied Materials, Inc. and Tokyo Electron, Ltd.

References

[1] Kawamura E, Lieberman M A, Lichtenberg A J 2006 *Phys. Plasmas* **13** 053506
[2] Bera K, Rauf S, Ramaswamy K and Collins K 2009 *J. Appl. Phys.* **106** 033301
[3] Georgieva V and Bogaerts A 2005 *J. Appl. Phys.* **98** 023308
[4] Donko Z and Petrovic Z Lj 2006 *Japan. J. Appl. Phys.* **45** 8151
[5] Chabert P 2007 *J. Phys. D: Appl. Phys.* **40** R63
[6] Lieberman M A, Booth J P, Chabert P, Rax J M and Turner M M 2002 *Plasma Sources Sci. Technol.* **11** 283
[7] Hebner G A, Barnat E V, Miller P A, Paterson A M and Holland J P 2006 *Plasma Sources Sci. Technol.* **15** 879
[8] Rauf S, Bera K and Collins K 2008 *Plasma Sources Sci. Technol.* **17** 035003
[9] Schmidt H, Sansonnens L, Howling A A, Hollenstein Ch, Elyaakoubi M and Schmitt J P M 2004 *J. Appl. Phys.* **95** 4559
[10] Ellingboe A R 2008 *US Patent* No 7,342,361
[11] Kushner M J 2009 *J. Phys. D: Appl. Phys.* **42** 194013
[12] Maloney J G, Shlager K L and Smith G S 1994 *IEEE Trans. Antennas Propag.* **42** 289
[13] Subramonium P and Kushner M J 2002 *J. Vac. Sci. Technol.* A **20** 313
[14] Koshiishi A, Araki Y, Himori S and Iijima T 2001 *Japan. J. Appl. Phys.* **40** 6613